InSb-Based Heterostructures for Electronic Device Applications

Michael Santos

Homer L. Dodge Department of Physics & Astronomy

University of Oklahoma

Norman, OK 73019 USA

Funded by NSF DMR-0808086 and DMR-0520550

Collaborators at Oklahoma

MBE Growth and Characterization: Madhavie Edirisooriya, Tetsuya Mishima, Chomani Gaspe, Mukul Debnath

Transmission Electron Microscopy: Tetsuya Mishima

Cyclotron Resonance: James Coker, Ryan Doezema

Ballistic Transport: Ruwan Dedigama, Sheena Murphy

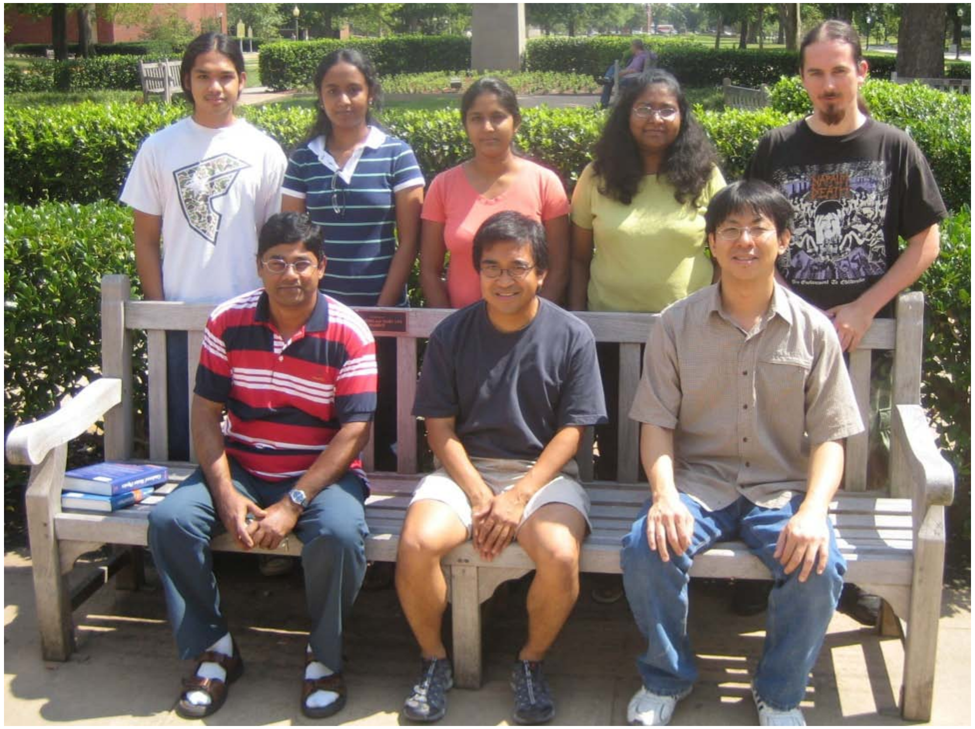

Bandgap versus Lattice Constant for III-V Materials

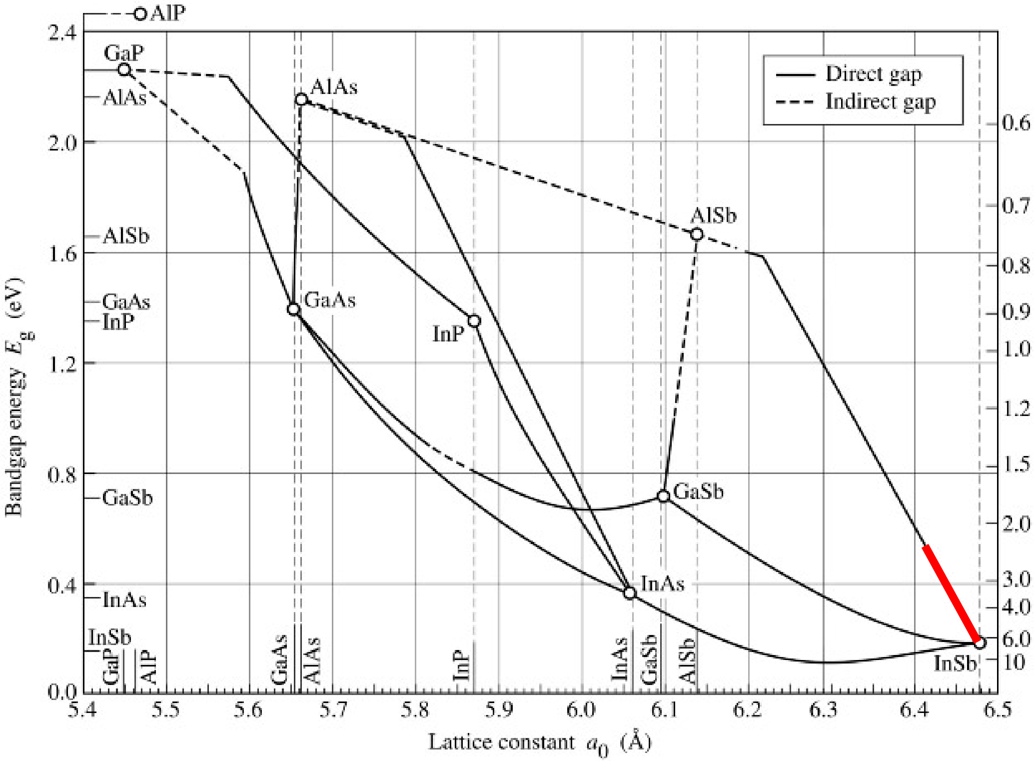

Fig. 7.6. Bandgap energy and lattice constant of various III-V semiconductors at room temperature (adopted from Tien, 1988).

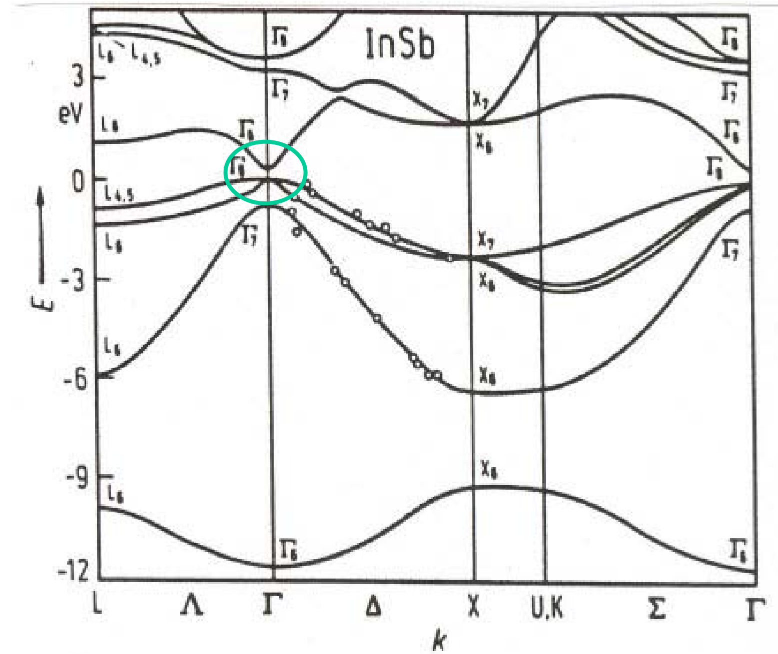

	electron m*	*g*-factor	E(k)
GaAs	0.067m$_o$	-0.5	least non-parabolic
InAs	0.023m$_o$	-15	more non-parabolic
InSb	0.014m$_o$	-51	most non-parabolic

InSb Quantum Well Field-Effect Transistors

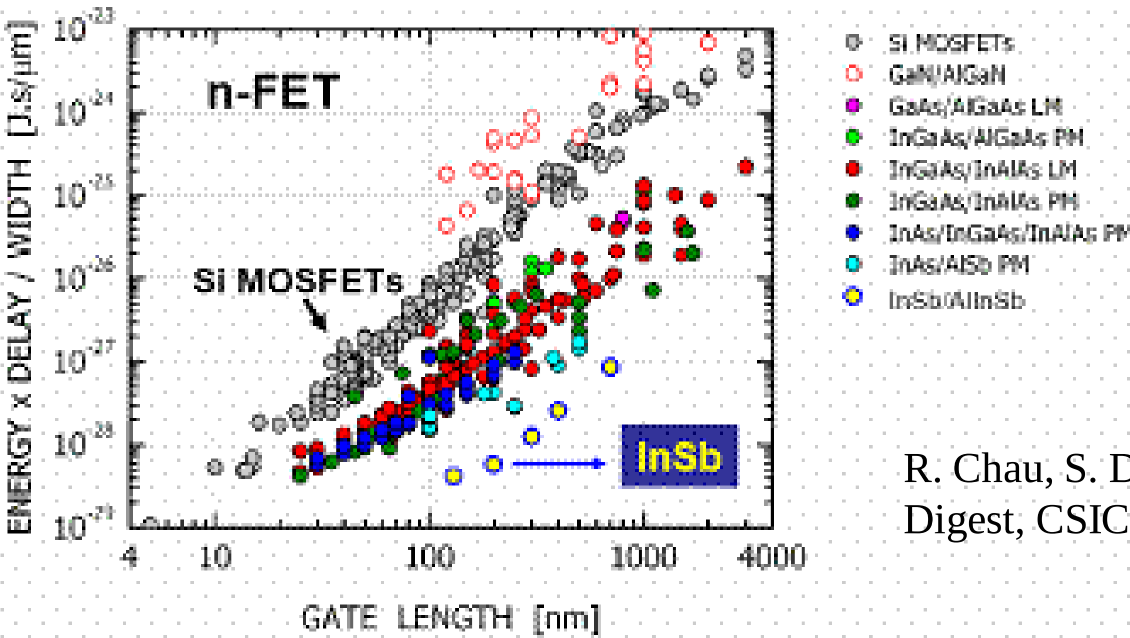

R. Chau, S. Datta, A. Mujumdar, Technical Digest, CSICS 2005, pp. 17-20.

Achievements

- Fabricated by Intel from InSb/$Al_xIn_{1-x}Sb$ material grown by QinetiQ
- For ultra high speed, very low power digital logic applications
- Takes advantage of high mobility and high saturation velocity for electrons in InSb quantum wells

Challenges

- Stable and reliable gate dielectrics for III-V semiconductors
- Integration of III-V devices on Si substrates
- *p*-channel III-V FET for CMOS configurations
- New logic/memory circuits and architecture (?)

InSb Quantum Wells for Mesoscopic Applications

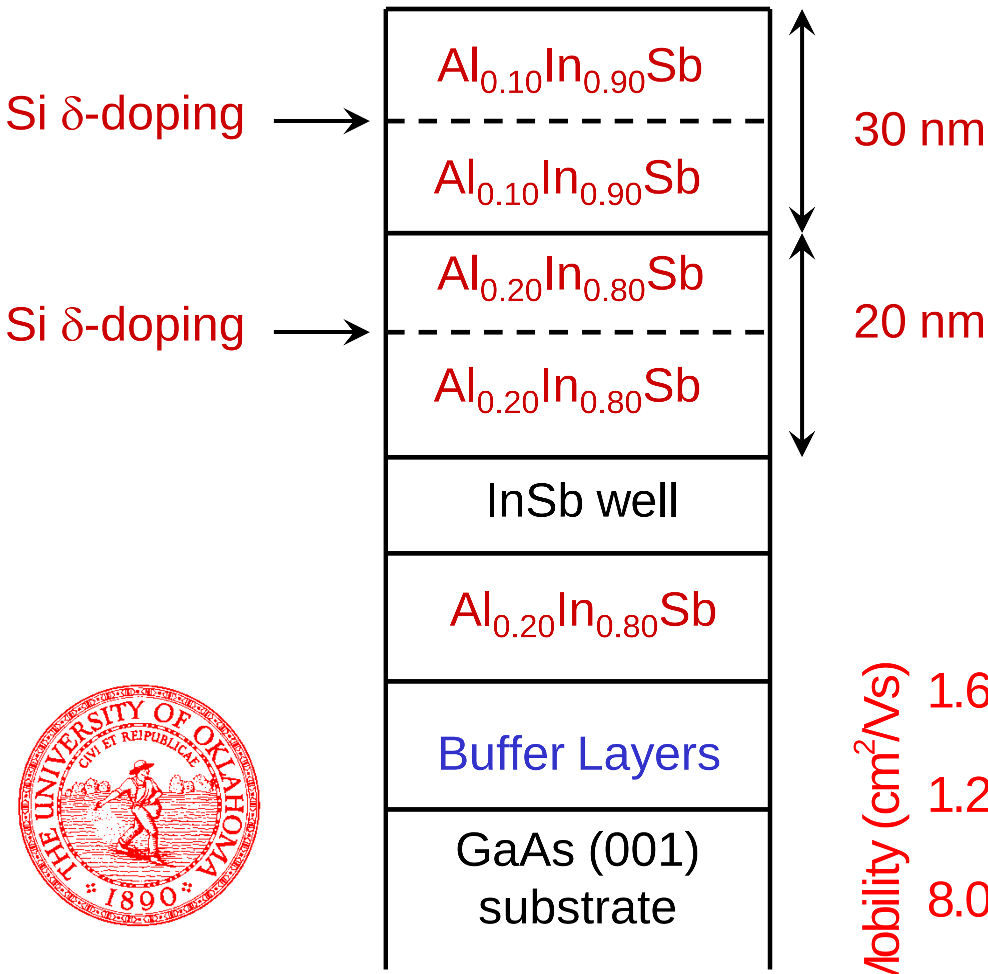

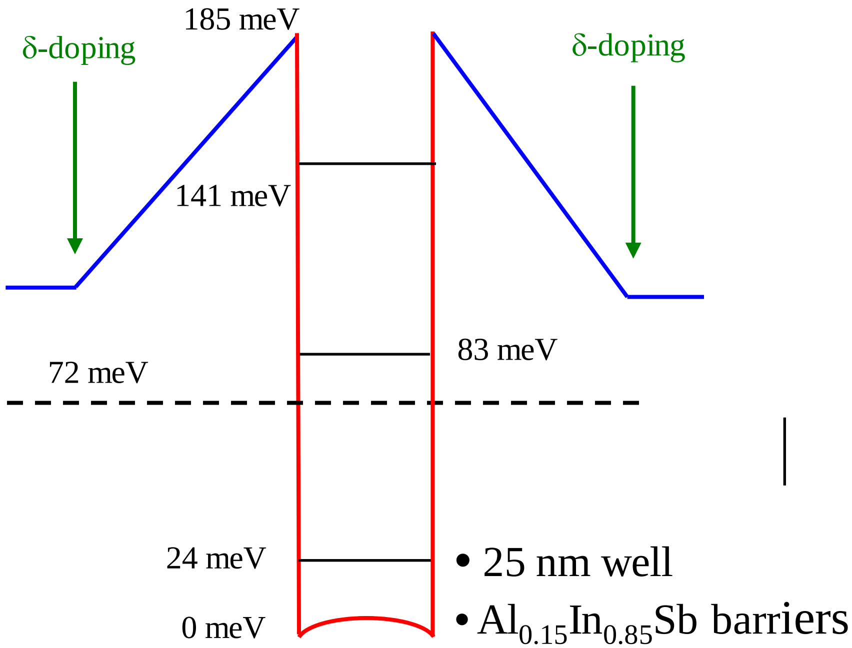

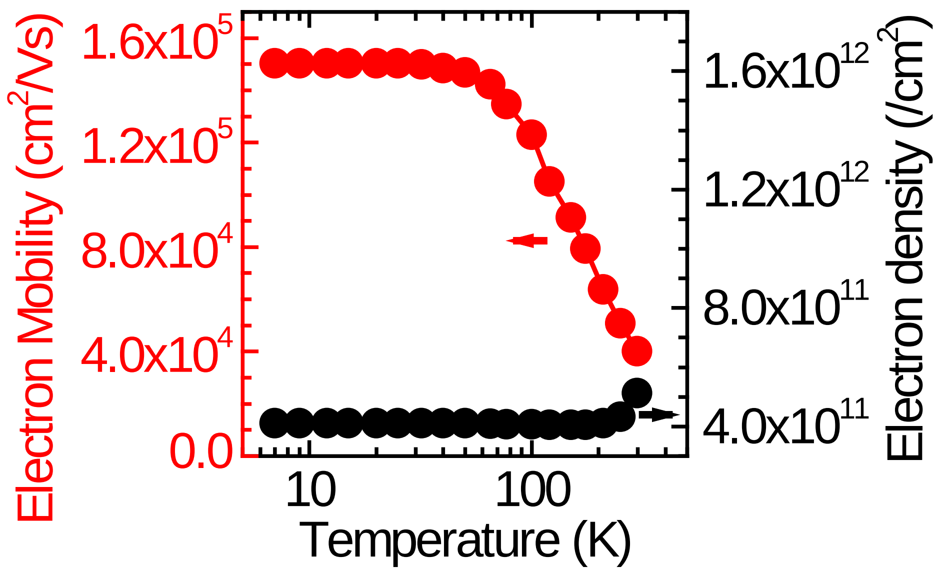

Grown by
Molecular Beam Epitaxy

Outline

1. **Introduction**

2. **Transmission Electron Microscopy**
• Effect of Crystalline Defects on Electron Mobility
• Effect of Buffer Layer on Defect Densities

3. **Transport Experiments on 2D Electron Systems**
• Quantum Hall Effect
• Quantized Conductance in Wires
• Magnetic Focusing

4. **Realization of 2D Hole Systems**
• Transport properties
• Cyclotron resonance

5. **Summary**

Defect Evaluation by Cross-sectional TEM (X-TEM)

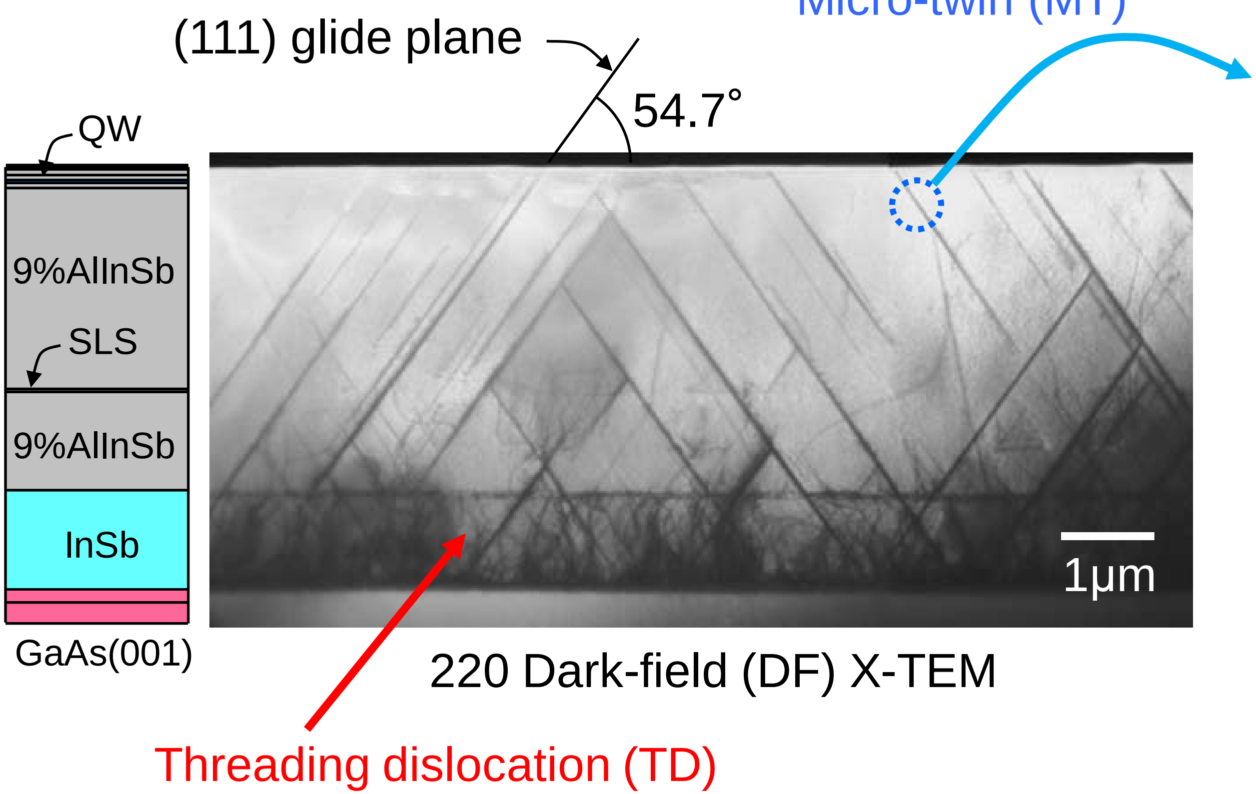

220 Dark-field (DF) X-TEM

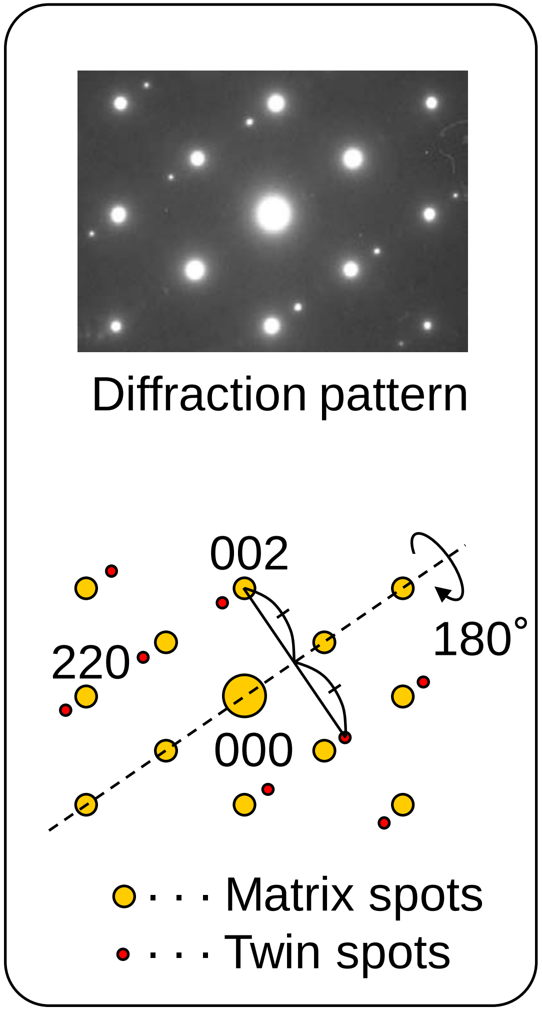

$Al_xIn_{1-x}Sb \rightarrow (x \times 100)\%AlInSb$

T.D. Mishima, M.B. Santos *et al.*, J. Cryst. Growth **251**, 551 (2003).

Formation of Misfit Dislocations

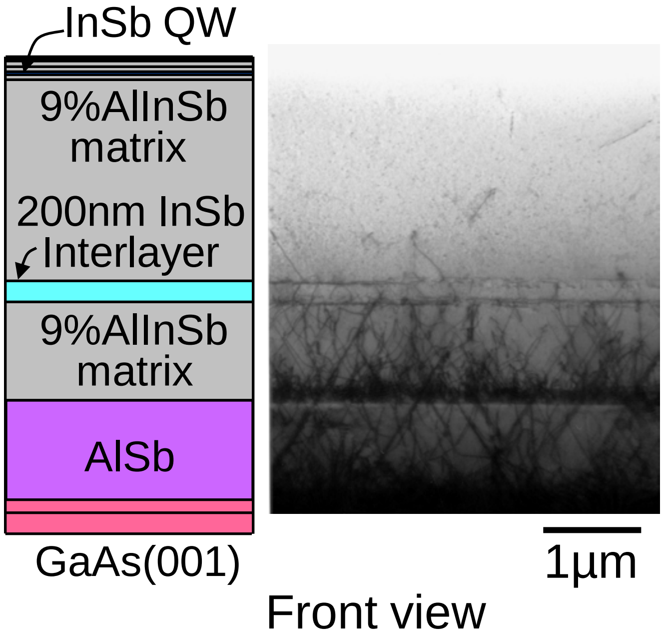

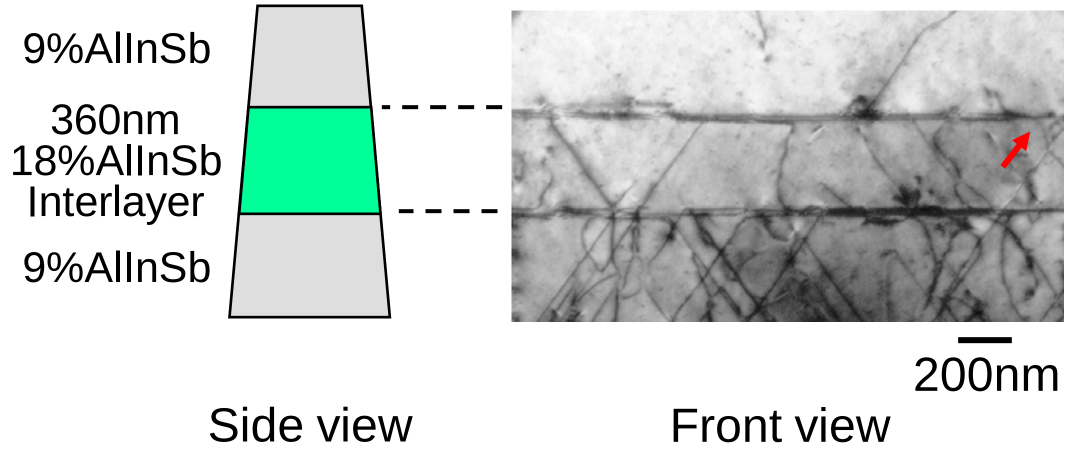

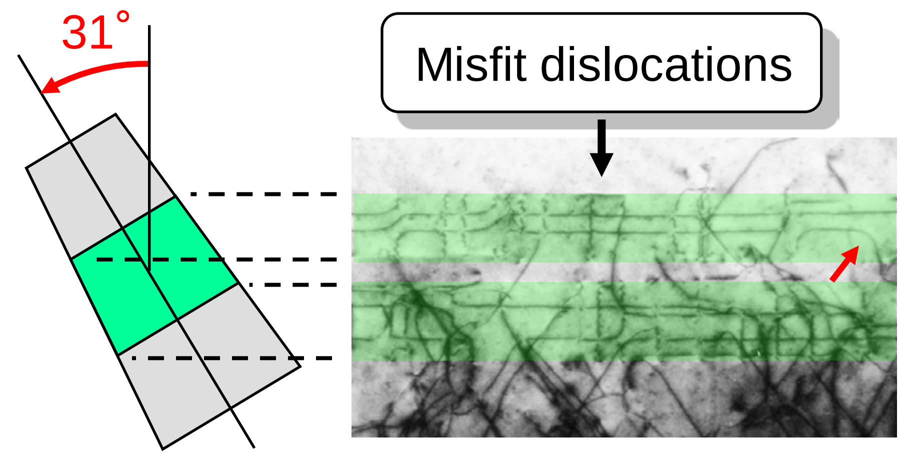

Lattice mismatch
with 9%AlInSb

InSb → + 0.5%

18%AlInSb → – 0.5%

Threading dislocations can change into a misfit dislocation at interfaces.

T.D. Mishima and M.B. Santos, J. Vac. Sci. Technol. **B22**, 1472 (2004).
T.D. Mishima, M. Edirisooriya, and M.B. Santos, Appl. Phys. Lett. **88**, 191908 (2006).

Dislocation Filtering Mechanism

Bending of pre-existing threading dislocations [1]

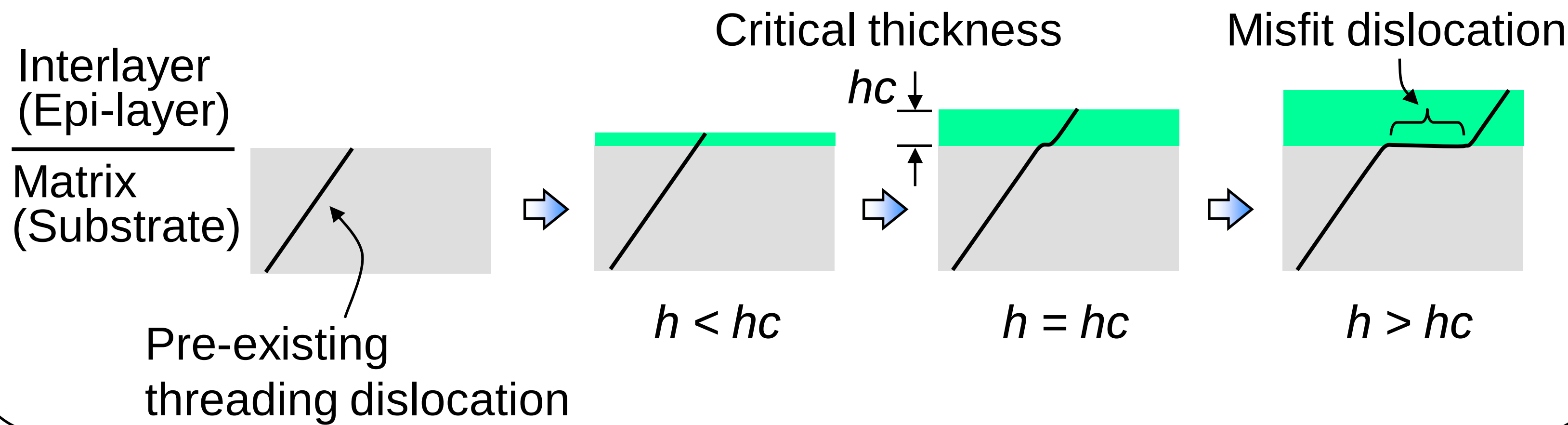

Lateral movement of TDs

→ Defect filtering

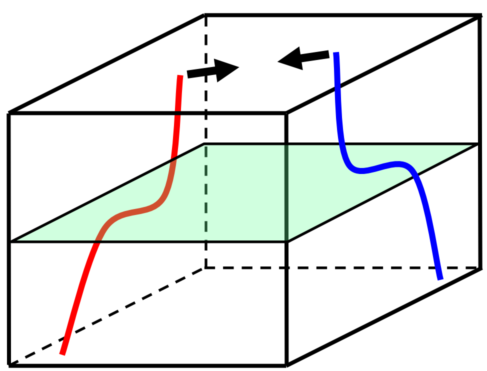

Dislocation filtering [2]

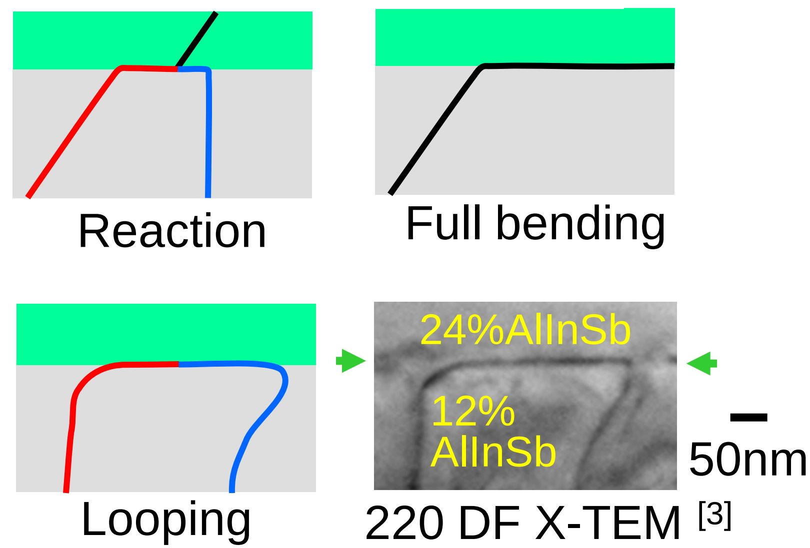

[1] J.W. Matthews and A.E. Blakeslee, J. Cryst. Growth **27**, 118 (1974).
[2] N.A. El-Masry *et al.*, J. Appl. Phys. **64**, 3672 (1988): Observed in strained-layer superlattice (SLS).
[3] T.D. Mishima *et al.*, to be published.

Effect of Interlayers on Threading Dislocations (TDs)

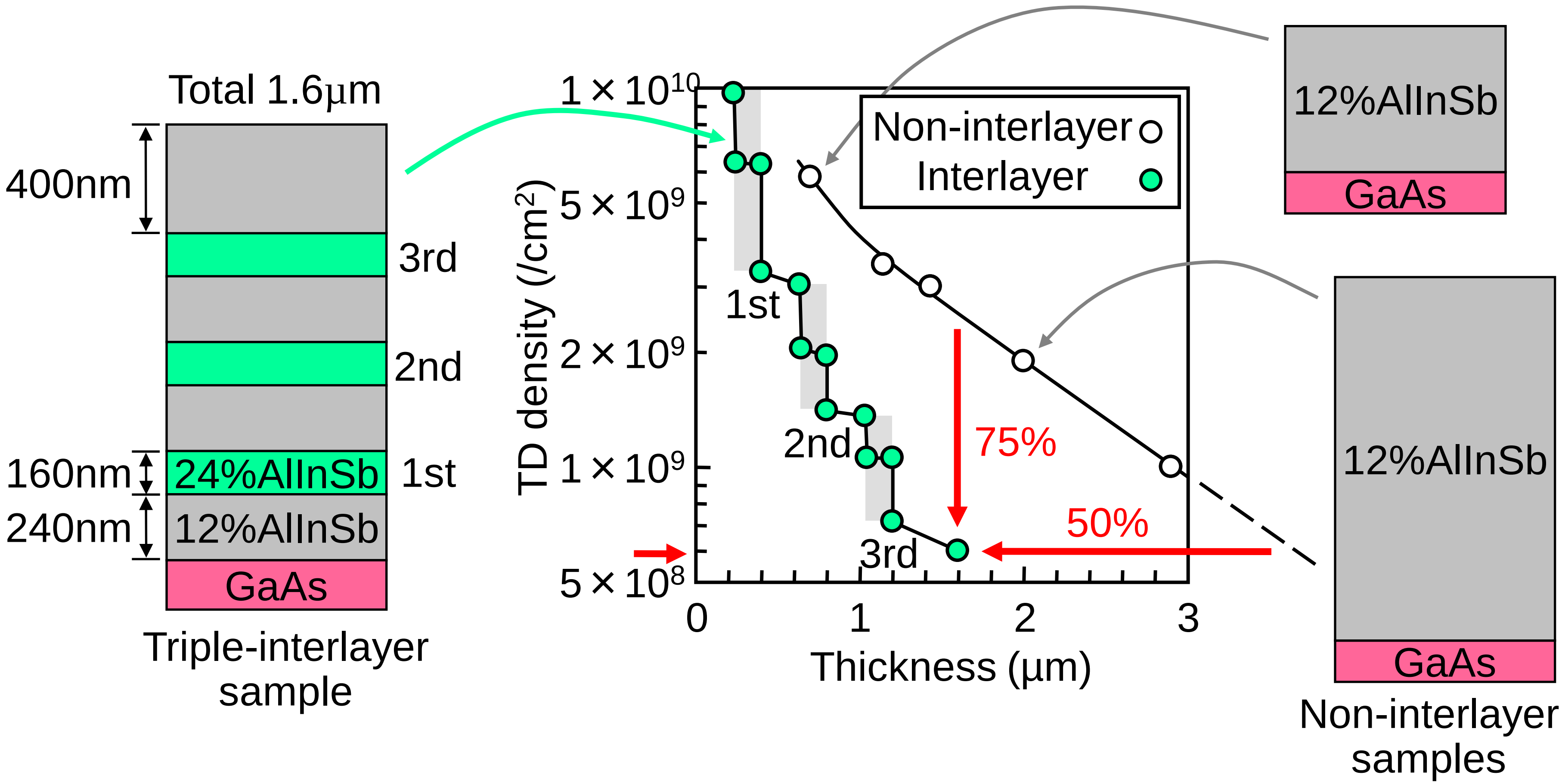

$Al_xIn_{1-x}Sb/Al_yIn_{1-y}Sb$ interlayers can be used to improve the performance of any InSb- (InAsSb)-based devices in which $Al_xIn_{1-x}Sb$ is used as a buffer, insulating, or barrier layer material.

T.D. Mishima *et al.*, Appl. Phys. Lett. **88**, 191908 (2006).

Effect of Micro-twin on InSb Quantum Well

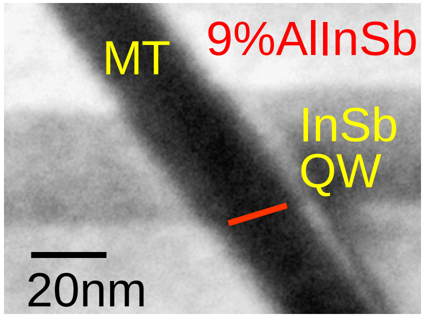

002 DF X-TEM [1]

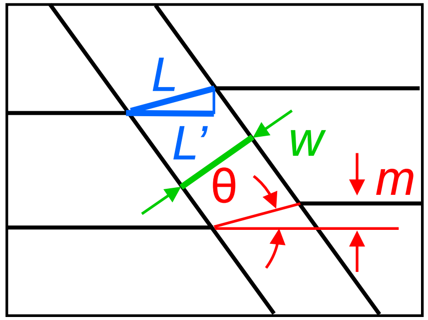

Geometrical relation [2]

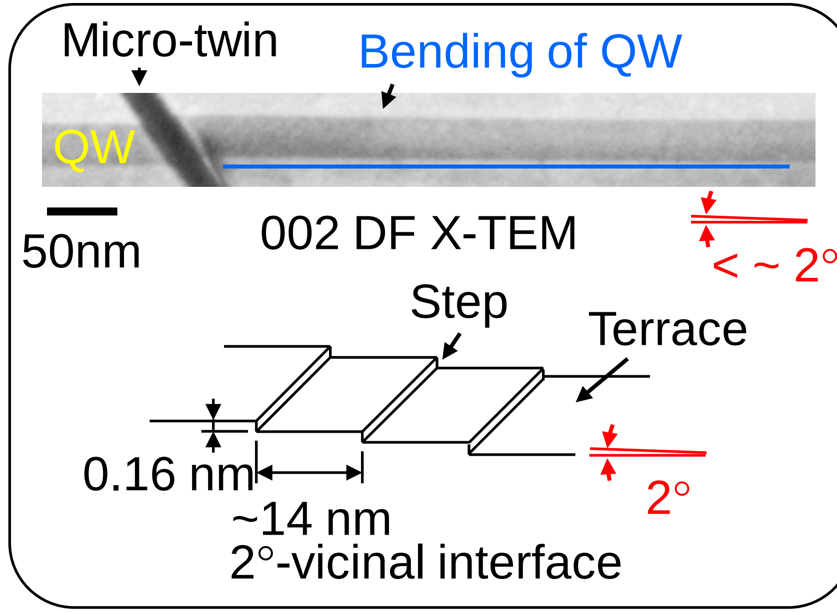

$$m = \frac{\sqrt{3}\sin\theta}{\sin\theta + \sqrt{2}\cos\theta} \times w$$

$$L = \frac{\sqrt{3}}{\sin\theta + \sqrt{2}\cos\theta} \times w \qquad L' = \frac{\sqrt{3}\cos\theta}{\sin\theta + \sqrt{2}\cos\theta} \times w$$

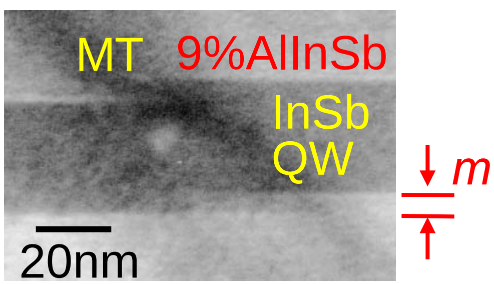

35°-tilted
002 DF X-TEM [2]

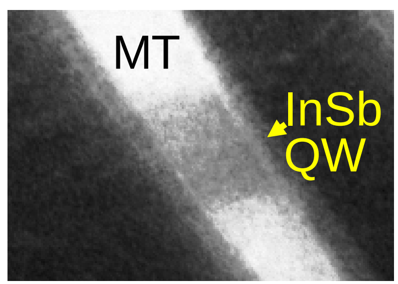

002_{MT} DF X-TEM [3]

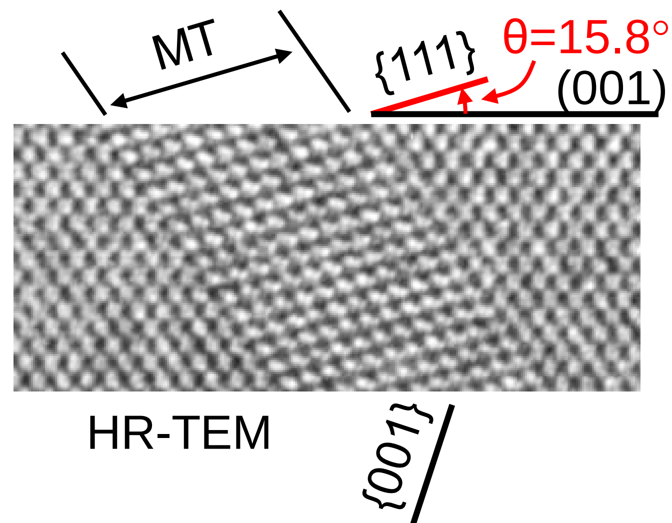

HR-TEM

[1] T.D. Mishima *et al.*, J. Cryst. Growth **251**, 551 (2003).
[2] T.D. Mishima *et al.*, Phys. Stat. Sol. (c) **5**, 2775 (2008).
[3] T.D. Mishima *et al.*, J. Vac. Sci. Technol. **B23**, 1171 (2005).

Electron Mobility and Structural Defects

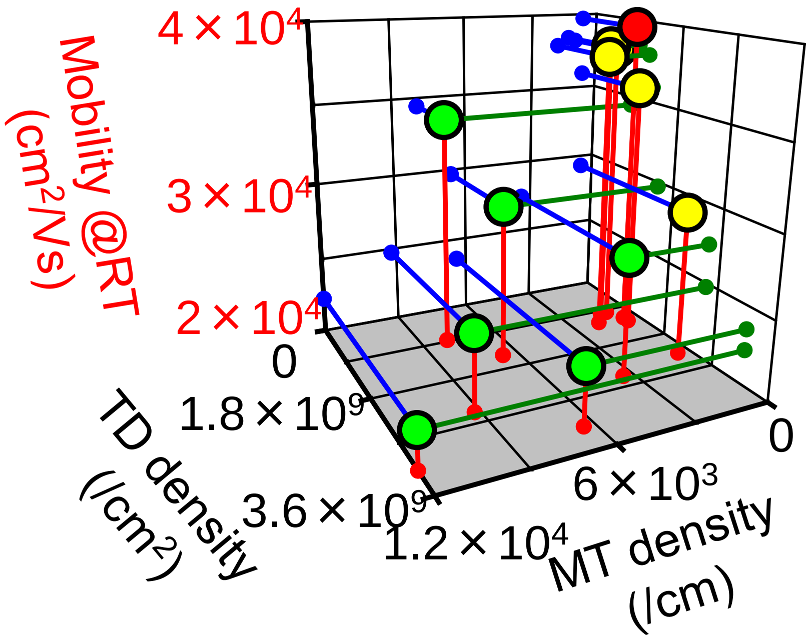

2° off-cut GaAs(001) [t_{QW} = 25nm]

2° off-cut GaAs(001) [t_{QW} = 20nm]

MT density 980 /cm

On-axis GaAs(001) [t_{QW} = 20nm] — 7,600 /cm

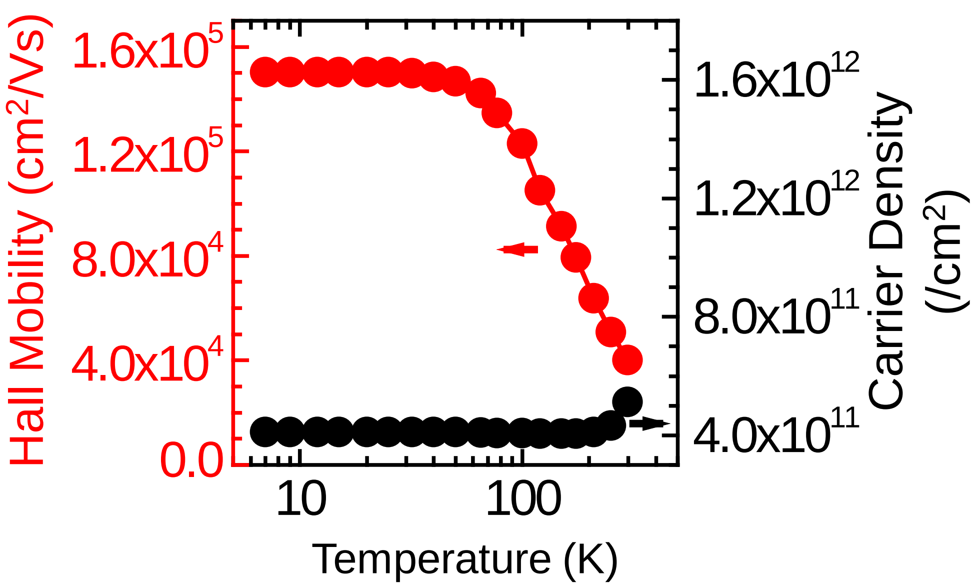

Electron Mobility in InSb QW @RT

30,000 → 41,000 cm^2/Vs (37%↑)

($n = 5.5 \times 10^{11}/cm^2$)

T.D. Mishima *et al*., Appl. Phys. Lett. **91**, 062106 (2007).

Summary of Defect Studies

- Mobility partially limited by threading dislocations and micro-twin defects
- Threading dislocations reduced by interlayers in the buffer layer
- Micro-twin density reduced by growth on off-axis substrates

Outline

1. **Introduction**

2. **Transmission Electron Microscopy**
- Effect of Crystalline Defects on Electron Mobility
- Effect of Buffer Layer on Defect Densities

3. **Transport Experiments on 2D Electron Systems**
- Quantum Hall Effect
- Quantized Conductance in Wires
- Magnetic Focusing

4. **Realization of 2D Hole Systems**
- Transport properties
- Cyclotron resonance

5. **Summary**

Quantum Hall Effect in InSb

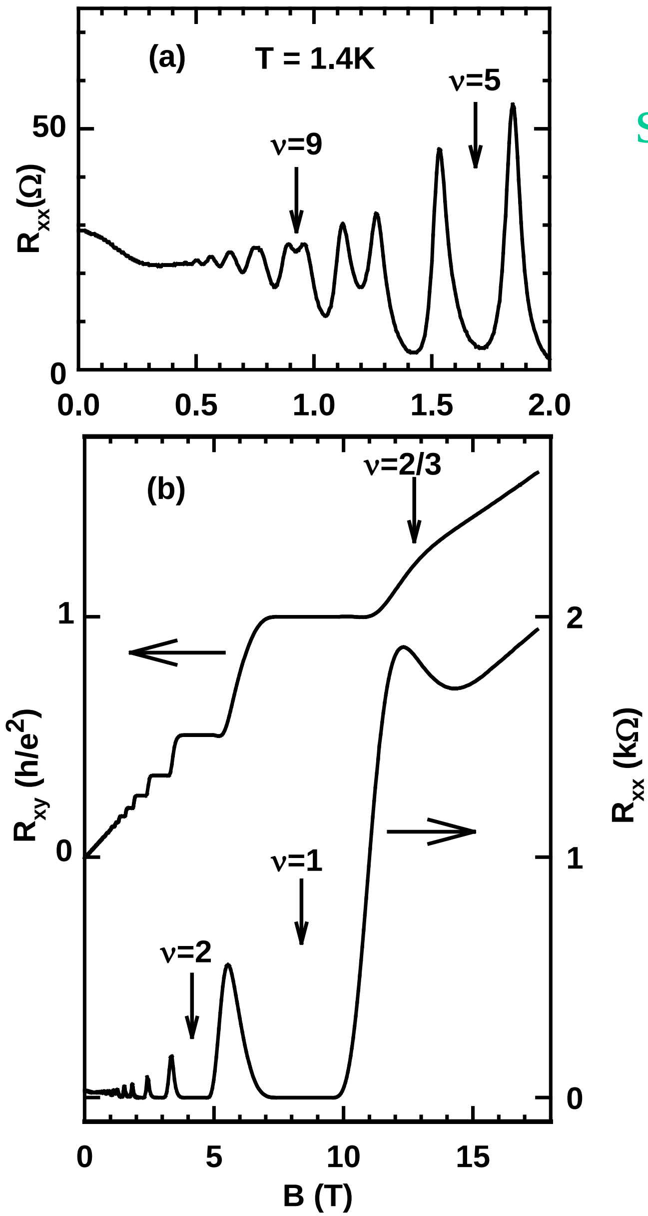

subband energy quantized orbits spin splitting

$$E_{i,n} = \boxed{E_i} + \boxed{\hbar\omega_c\left(n+\tfrac{1}{2}\right)} \boxed{\pm \tfrac{1}{2} g^* \mu_B B}$$

$$\omega_c = \frac{eB_\perp}{m^*} \qquad \mu_\mathrm{B} = \frac{e\hbar}{2m}$$

- Strong Integer QHE with Zeeman splitting resolved at low *B*
- Landau and Zeeman splittings equal at tilt of 65° for ν=2 (m^*g=0.84)
- Fractional QHE not observed

Quantum Point Contacts

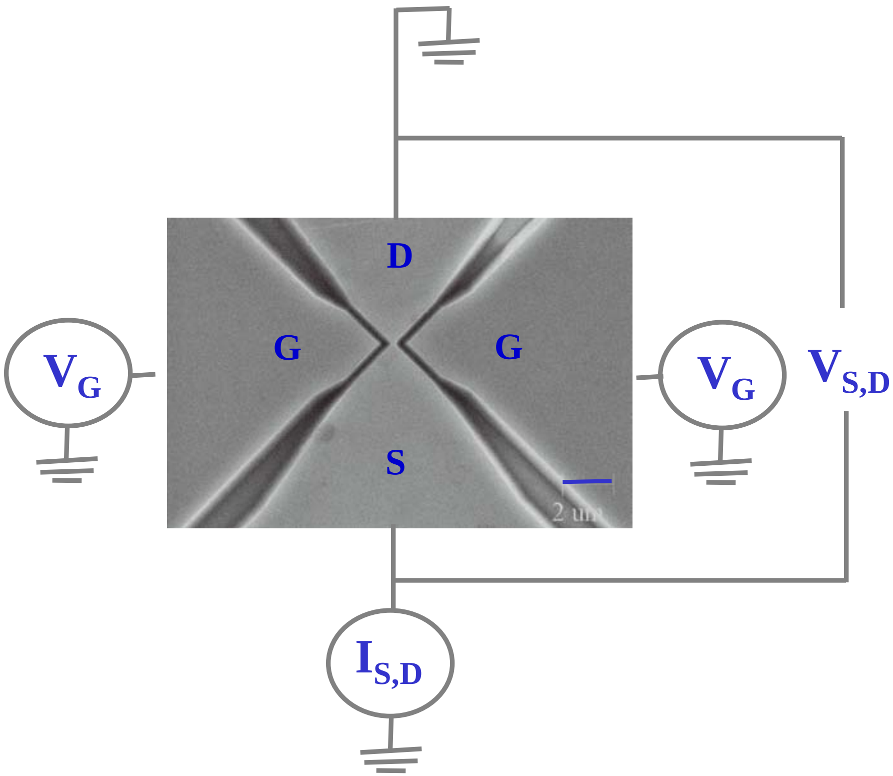

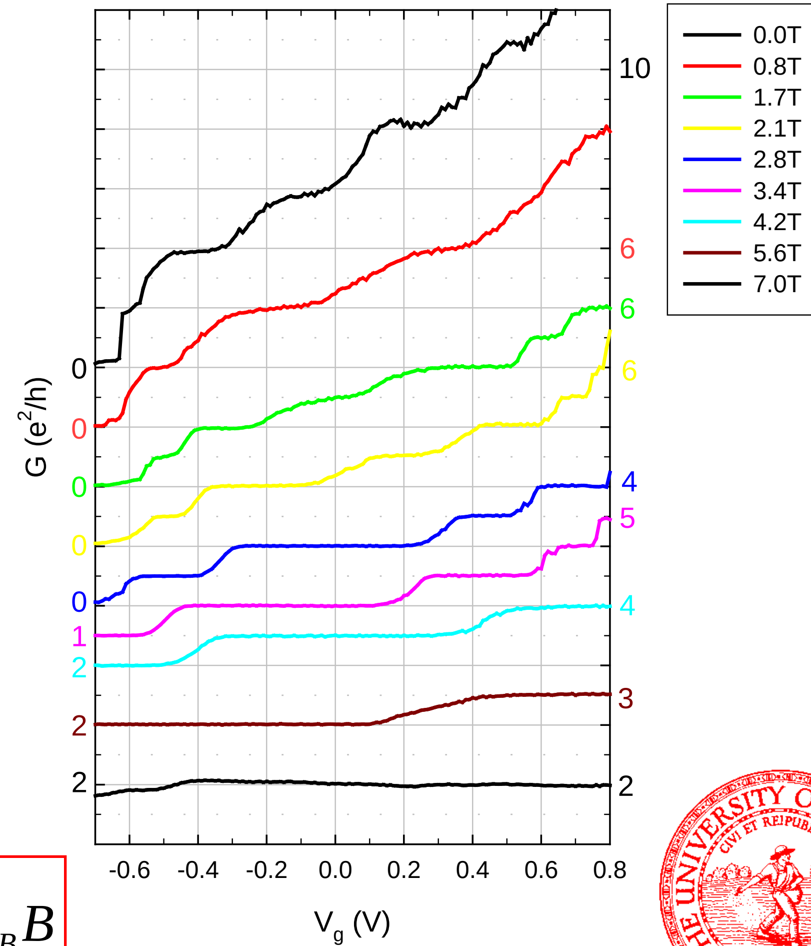

$$E_{m,n} = E_m + \left(n + \tfrac{1}{2}\right)\hbar\boxed{\omega} + \frac{\hbar^2 k_y^2}{2\boxed{M}} \boxed{\pm \tfrac{1}{2} g\mu_B B}$$

$$M = m^* \frac{\omega^2}{\omega_0^2}, \quad \omega = \sqrt{\omega_0^2 + \omega_c^2}, \quad \omega_c = \frac{eB}{m^*}$$

Increase B → Increase confinement → Level depopulation

Spin Orbit Effects

Bulk Inversion Asymmetry
(Dresselhaus splitting)

$$E=\frac{\hbar^2 k_{//}^2}{2m}\pm\eta\left[\left\langle k_z^2\right\rangle k_{//}-\frac{1}{2}k_{//}^3\sin^2(2\phi)+O\left(k_{//}^5\right)\right]$$

Structural Inversion Asymmetry
(Rashba splitting)

$$E=\frac{\hbar^2 k_{//}^2}{2m}\pm\alpha_0\left\langle E_z\right\rangle k_{//}$$

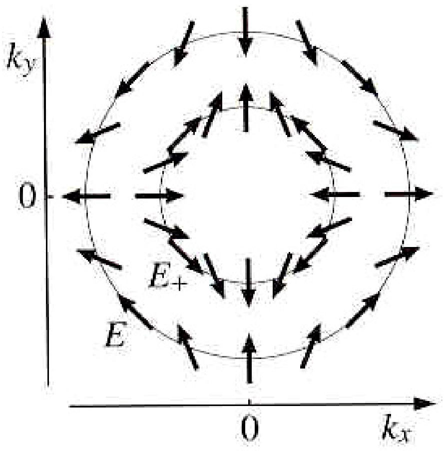

	η	**α**
GaAs	27.6 eV A^3	5.2 e A^2
InAs	27.2 eV A^3	117 e A^2
InSb	760 eV A^3	523 e A^2

R. Winkler, Springer Tracts in Modern Physics 191 (2004)

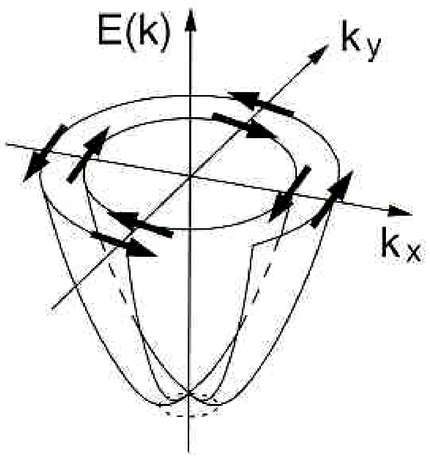

Spin-dependent trajectories expected:

"Transverse electron focusing in systems with spin orbit coupling," Usaj and Balseiro, PRB 70, 041301 (2004)

"Spin separation in cyclotron motion," Rokhinson *et al.*, PRB 93, 146601 (2004)

"Spin-polarized reflection of electrons in a two-dimensional electron system," Chen *et al.*, APL 86, 032113 (2005)

APPLIED PHYSICS LETTERS 86, 032113 (2005)

Spin-polarized reflection in a two-dimensional electron system

Hong Chen, J. J. Heremans,[a] J. A. Peters, and A. O. Govorov
Department of Physics and Astronomy, and The Nanoscale and Quantum Phenomena Institute, Ohio University, Athens, Ohio 45701

N. Goel, S. J. Chung, and M. B. Santos
Department of Physics and Astronomy, and Center for Semiconductor Physics in Nanostructures, The University of Oklahoma, Norman, Oklahoma 73019

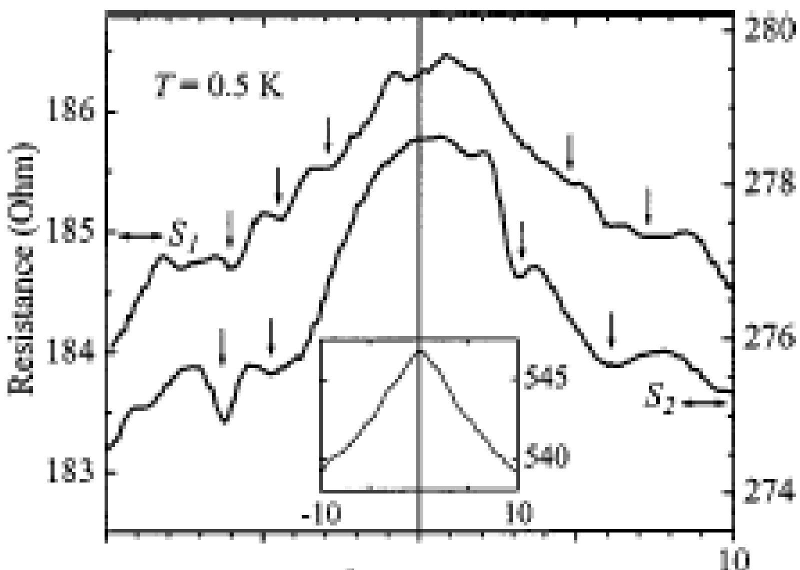

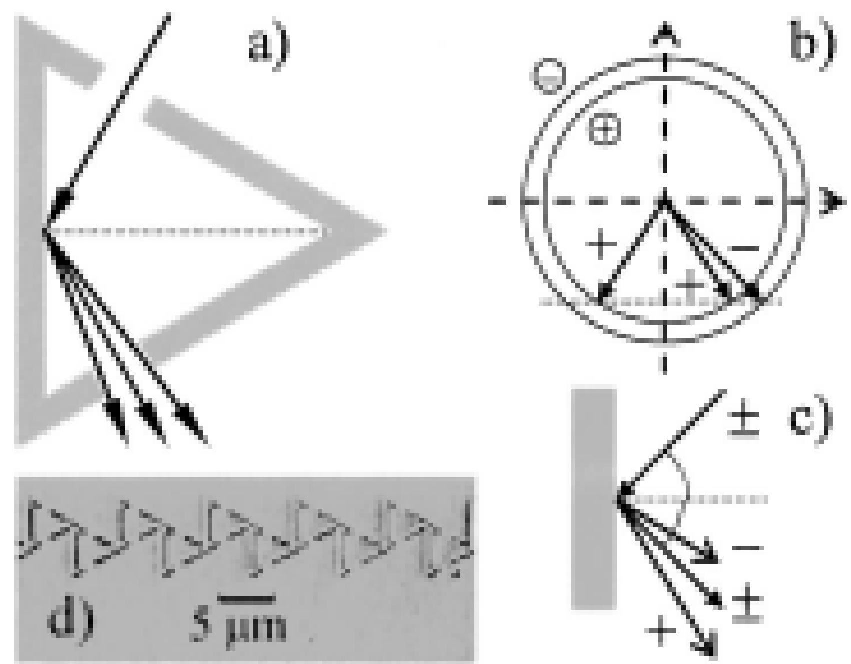

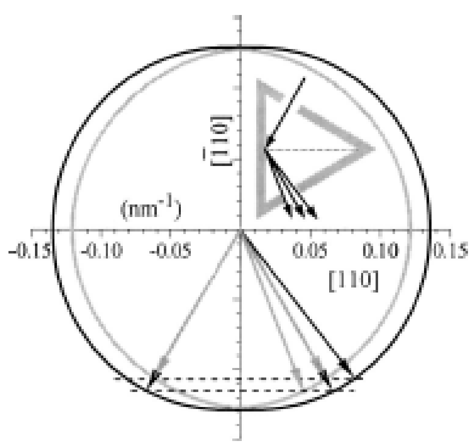

<u>Deduced values:</u>

Dresselhaus parameter, $\eta=7.6\times10^{-28}$ eV m

Rashba parameter, $\alpha=1.0\times10^{-11}$eV m

Magnetic Focusing Data

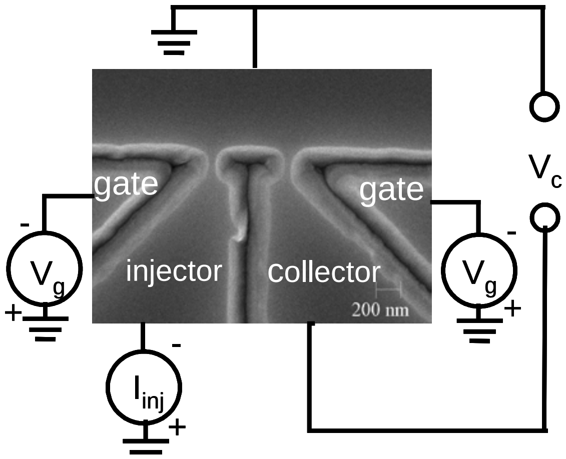

$$r_c = \frac{v_f}{\omega_c} = \frac{\hbar}{eB}\sqrt{2\pi n_s}$$

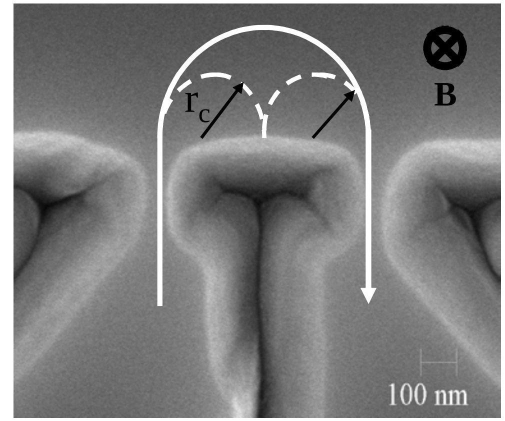

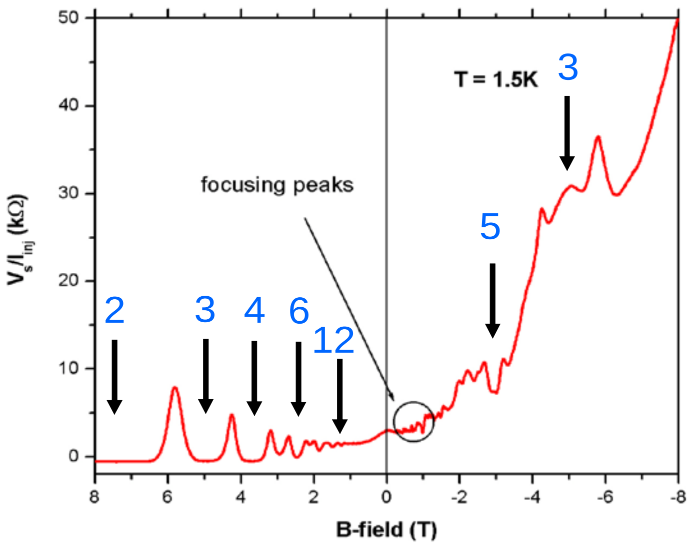

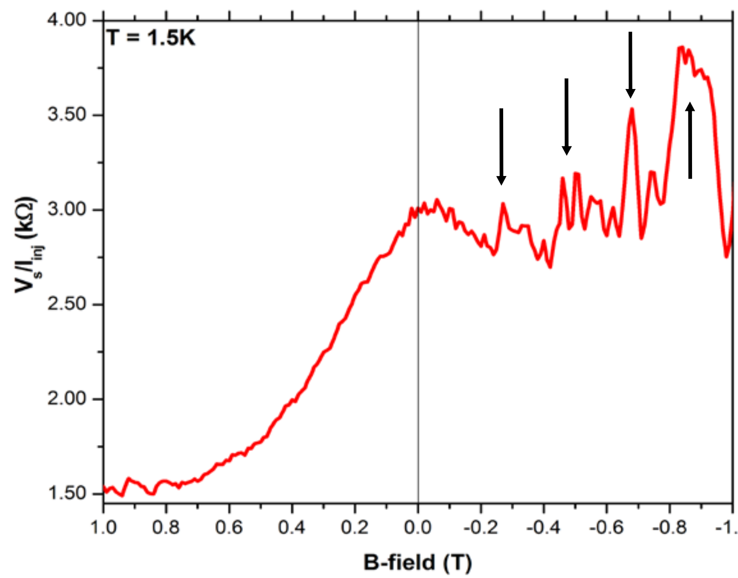

- Shubnikov de Haas oscillations → $n_s = 3.62 \times 10^{11} cm^{-2}$
- Measured period of ≈0.2T implies L≈1.0μm

A.R. Dedigama *et al.*, Physica **E 34**, 647 (2006).

Summary of Ballistic Transport Experiments

- Ballistic transport observed at $T\sim 200K$ in 0.5μm devices
- Quantized conductance observed in point contacts
- Magnetic focusing features observed
- Goal: Spin-dependent transport devices

Outline

1. **Introduction**

2. **Transmission Electron Microscopy**
- Effect of Crystalline Defects on Electron Mobility
- Effect of Buffer Layer on Defect Densities

3. **Transport Experiments on 2D Electron Systems**
- Quantum Hall Effect
- Quantized Conductance in Wires
- Magnetic Focusing

4. **Realization of 2D Hole Systems**
- Transport properties
- Cyclotron resonance

5. **Summary**

Two-Dimensional Hole Systems in III-V Materials

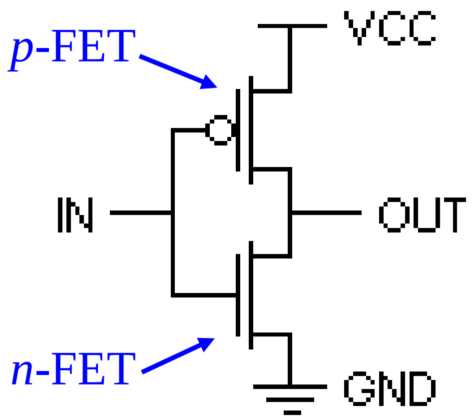

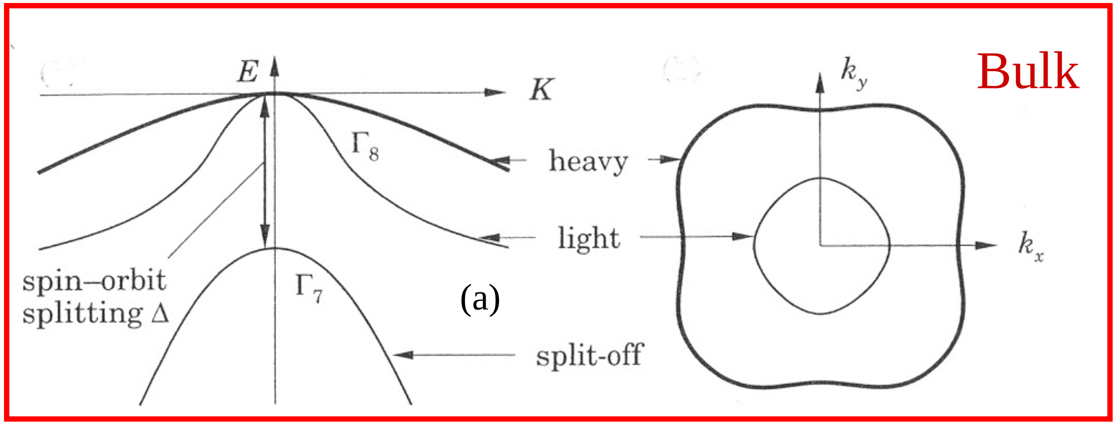

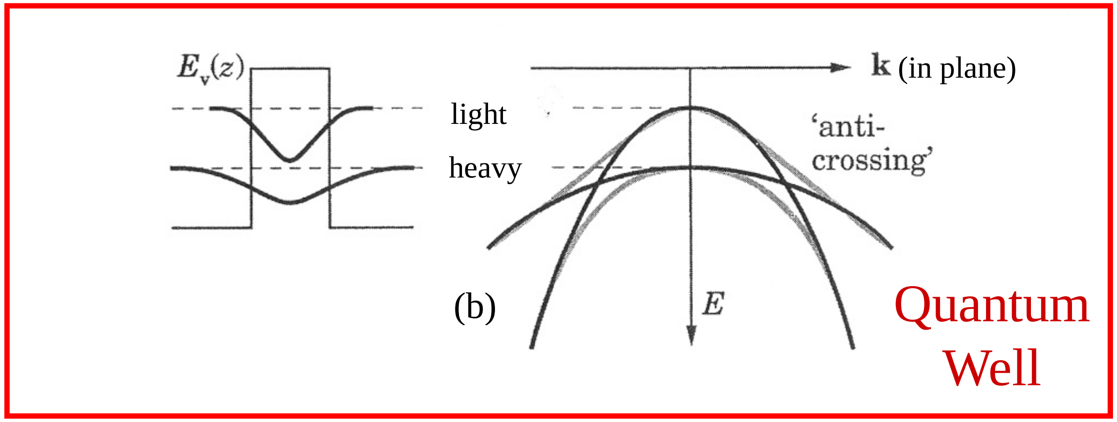

- In-plane hole masses are anisotropic
- Degeneracy of "light" and "heavy" holes lifted by strain and confinement
- "Light" holes have heavy in-plane mass, "heavy" holes have light in-plane mass
- Anticrossing expected between "light" and "heavy" hole bands

The Physics of Low-Dimensional Electron Systems by John H. Davies (1998).

p-type InSb Quantum Well

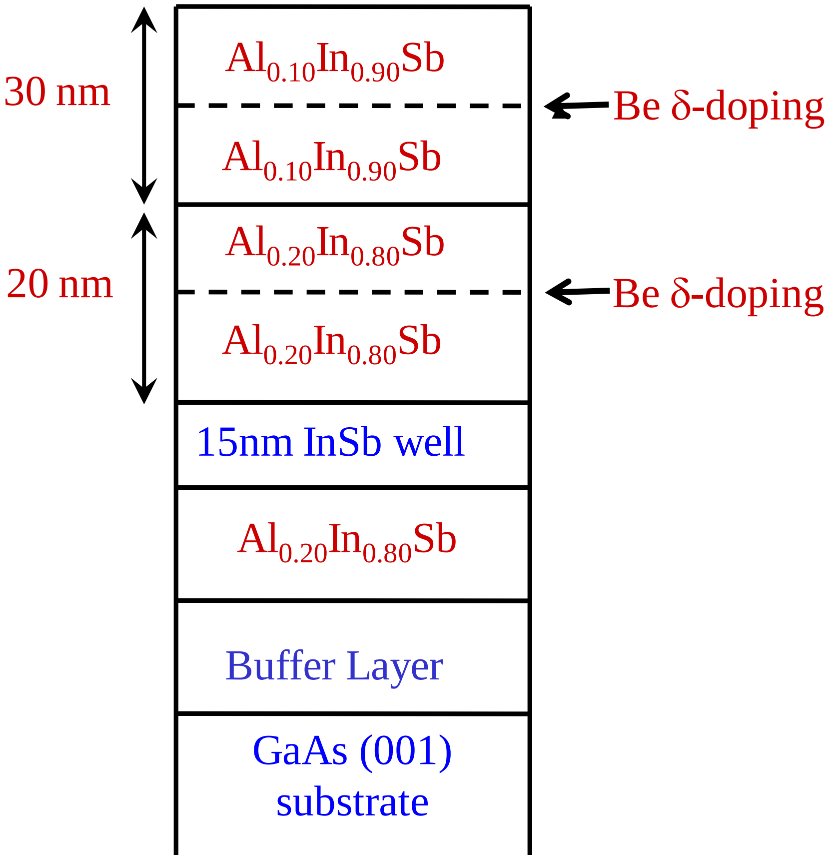

	μ_H at 300K	Reference
$In_{0.2}Ga_{0.8}As$	260 cm^2/Vs	R.T. Hsu *et al.*, *Appl. Phys. Lett.* **66**, 2864 (1995).
$In_{0.53}Ga_{0.48}As$	265 cm^2/Vs	Y-J. Chen and D. Pavlidis, *IEEE Trans. Elec. Dev.* **39**, 466 (1992).
$In_{0.82}Ga_{0.18}As$	295 cm^2/Vs	A.M. Kusters *et al.*, *IEEE Trans. Elec. Dev.* **40**, 2164 (1993).
InSb	700 cm^2/Vs	M. Edirisooriya *et al.*, J. Crystal Growth (in press).
$In_{0.4}Ga_{0.6}Sb$	1500 cm^2/Vs	B.R. Bennett *et al.*, *Appl. Phys. Lett.* **91**, 042104 (2007).
Ge	3100 cm^2/Vs	M. Myronov, *Appl. Phys. Lett.* **91**, 082108 (2007).

- First realization of remotely-doped *p*-type InSb QWs.

p-type InSb Quantum Well at Low Temperature

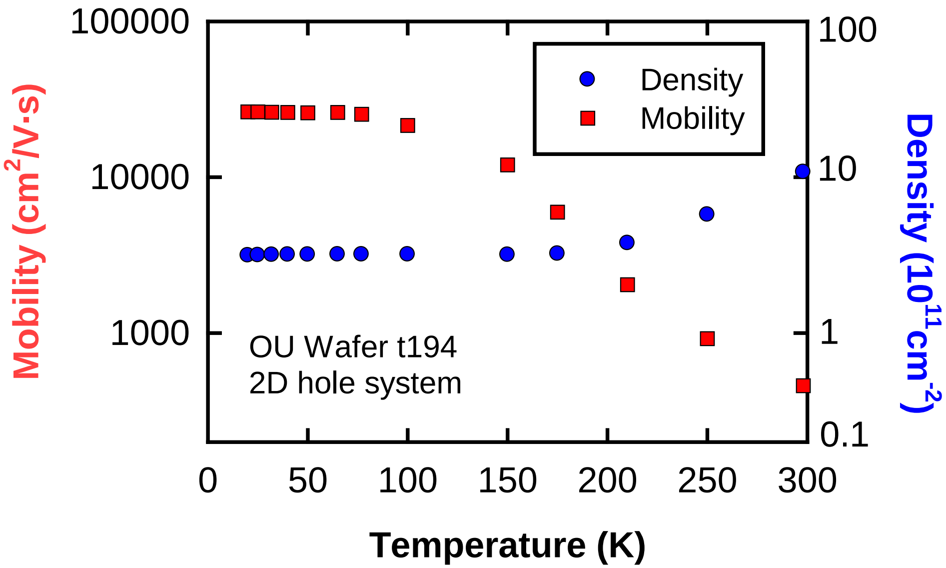

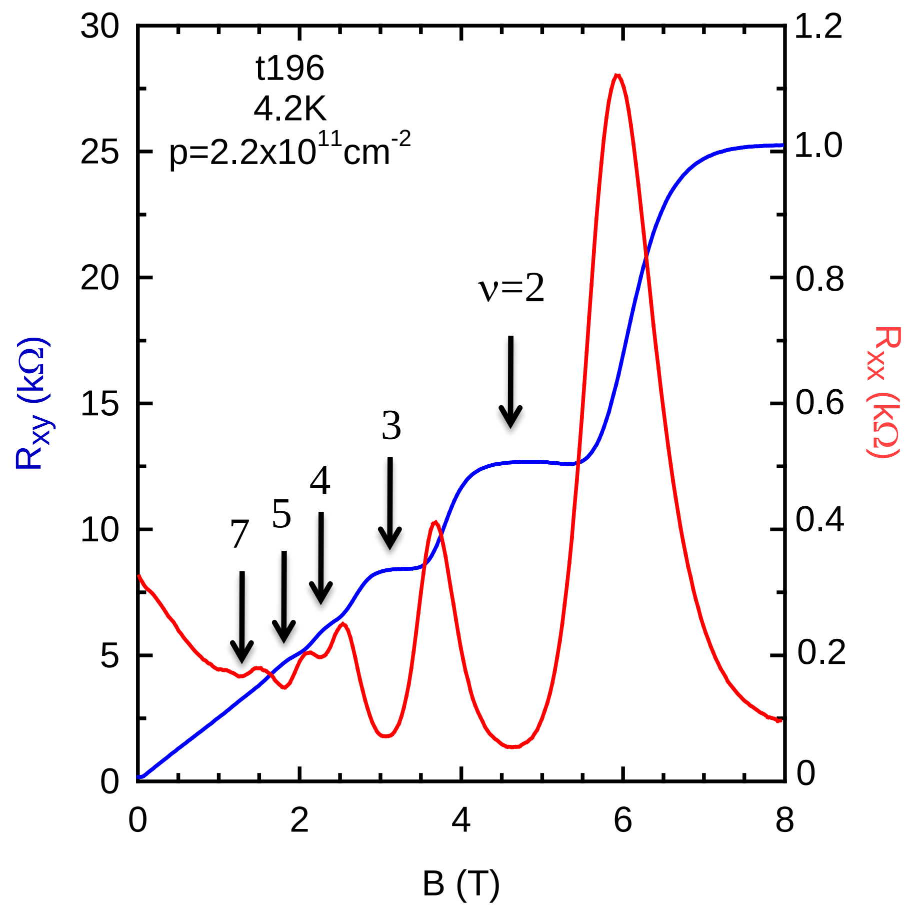

μ_h= 700 cm^2/Vs @300K (T250)
μ_h= 29,900 cm^2/Vs @77K (T241)
μ_h= 55,600 cm^2/Vs @20K (T241)

Mobility in *p*-type QW is ~3 (~55) times smaller at 25K (300K) than in *n*-type QW with same layer structure.

Spin Resolved Cyclotron Resonance in *n*-type InSb QW

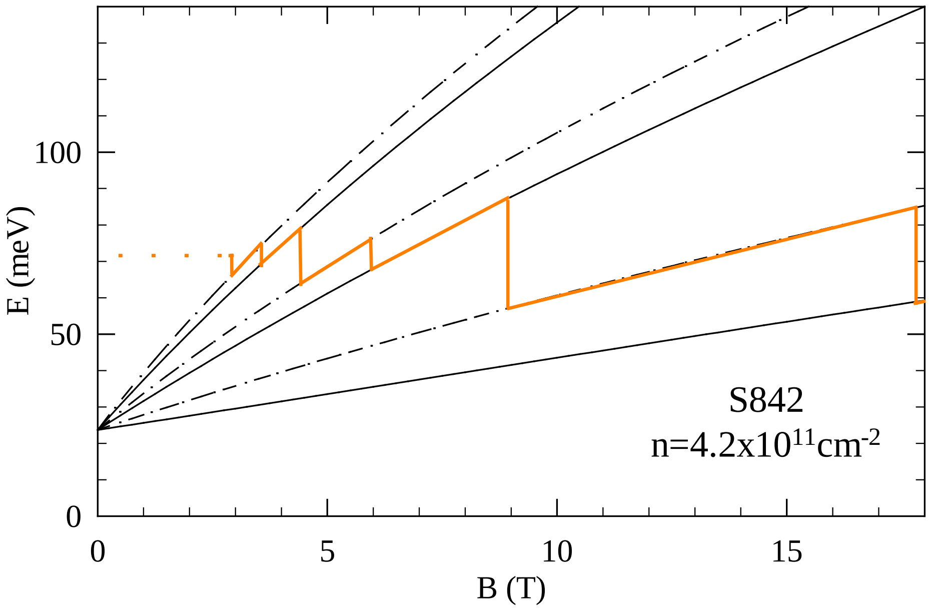

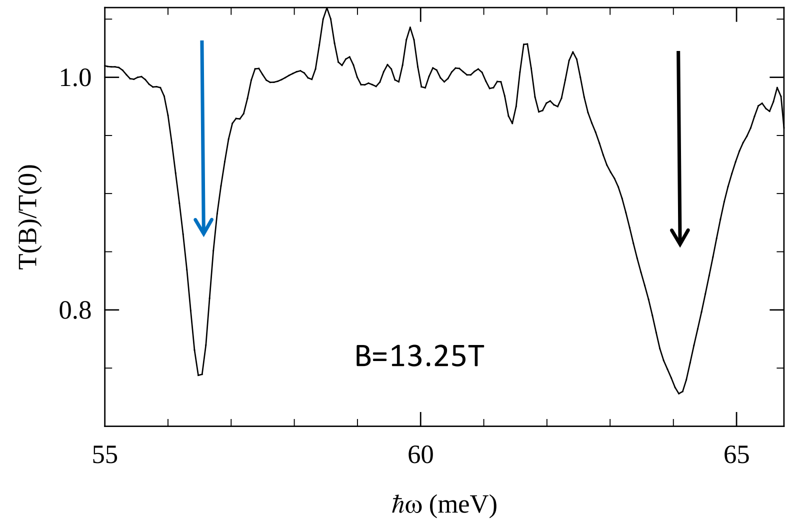

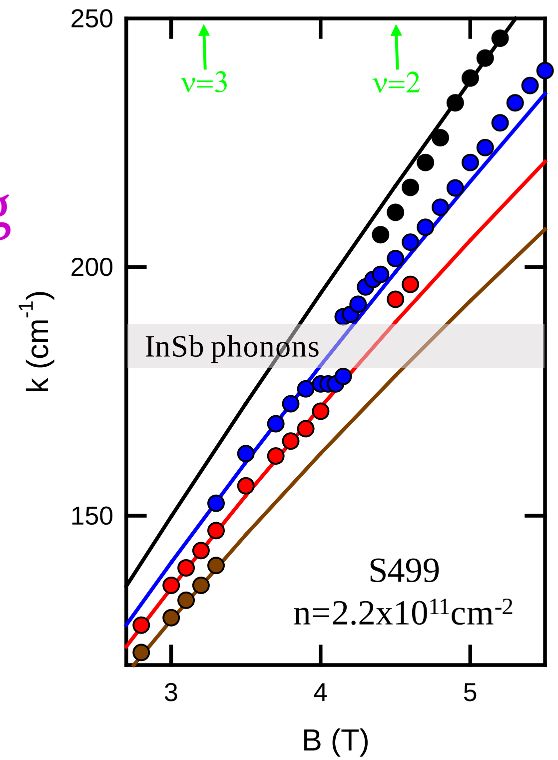

subband energy quantized orbits spin splitting

$$E_{i,n} = \boxed{E_i} + \boxed{\hbar\omega_c\left(n+\tfrac{1}{2}\right)} \boxed{\pm \tfrac{1}{2} g^* \mu_B B}$$

$$\omega_c = \frac{eB_\perp}{m^*} \qquad \mu_\mathrm{B} = \frac{e\hbar}{2m}$$

Modeling of Landau Levels in InSb QW

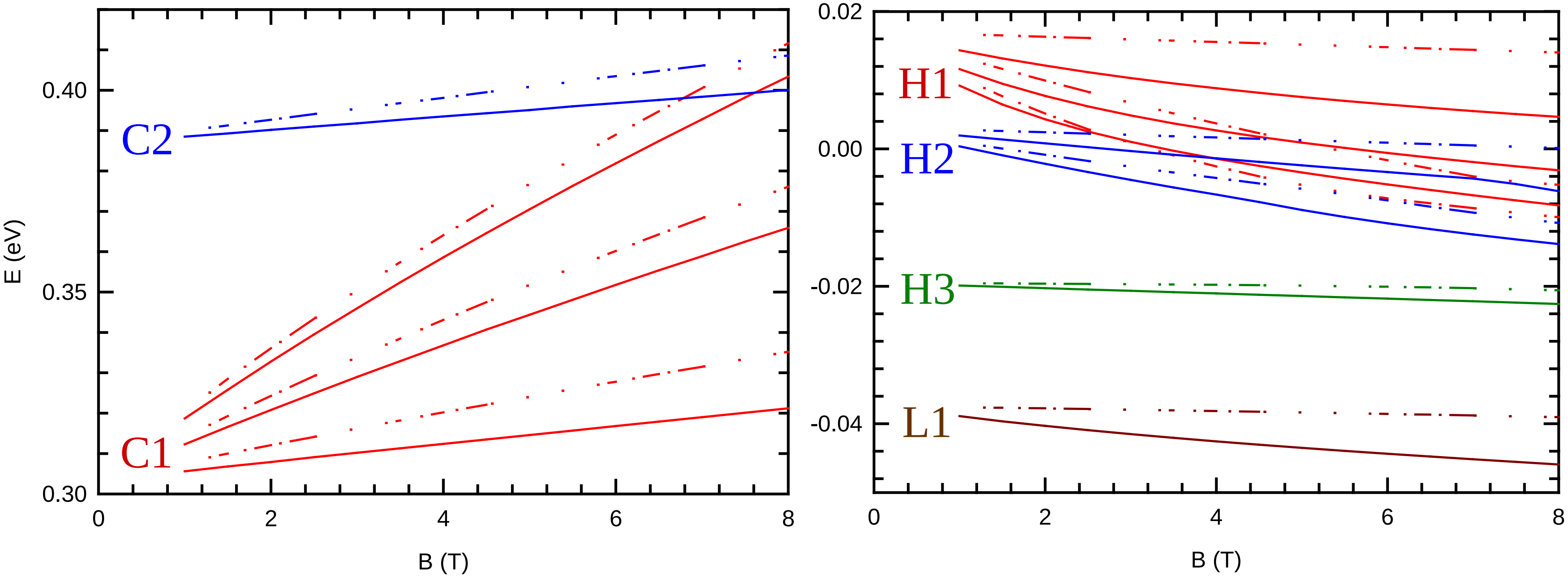

- Narrow Gap ⇒ *conduction band/valence band mixing* ⇒ 8 band k•p *effective mass* approximation (Pidgeon-Brown + k_z + confinement).
- Superlattice/MQW effects using Finite Difference method.
- Band gap discontinuities & strain effects included.
- Magneto-Optics using Fermi's Golden Rule.
- Material Parameters from experimental measurements.

UNIVERSITY of FLORIDA

Spin Resolved Cyclotron Resonance in *p*-type InSb QW

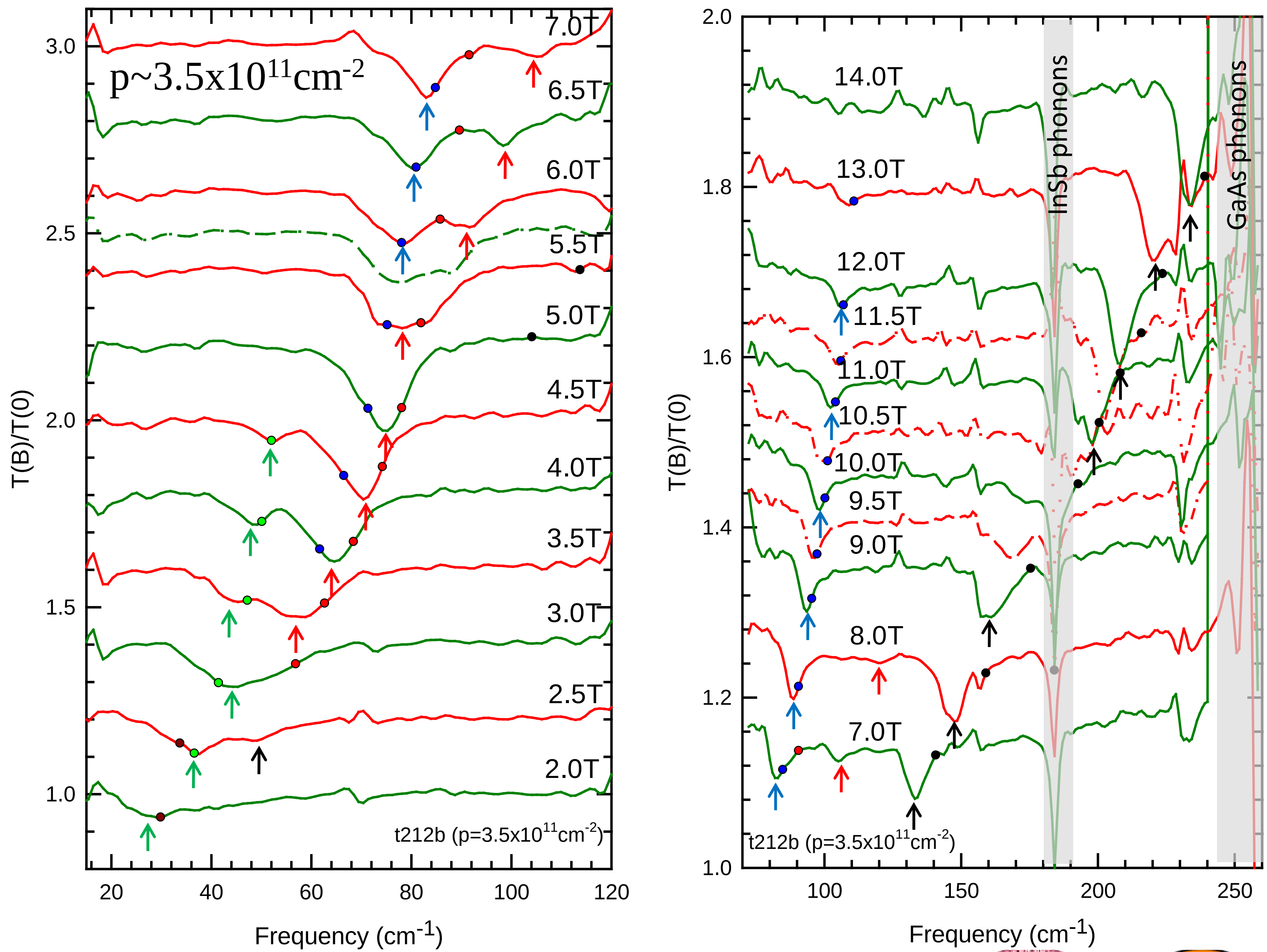

CR across wide range of B

CR in *p*-type InSb Quantum Well

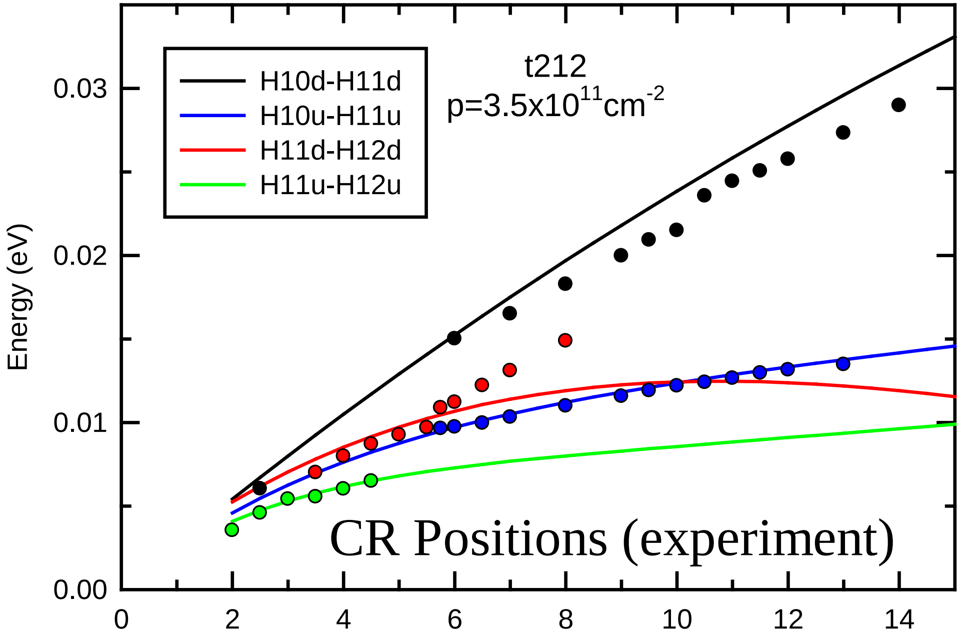

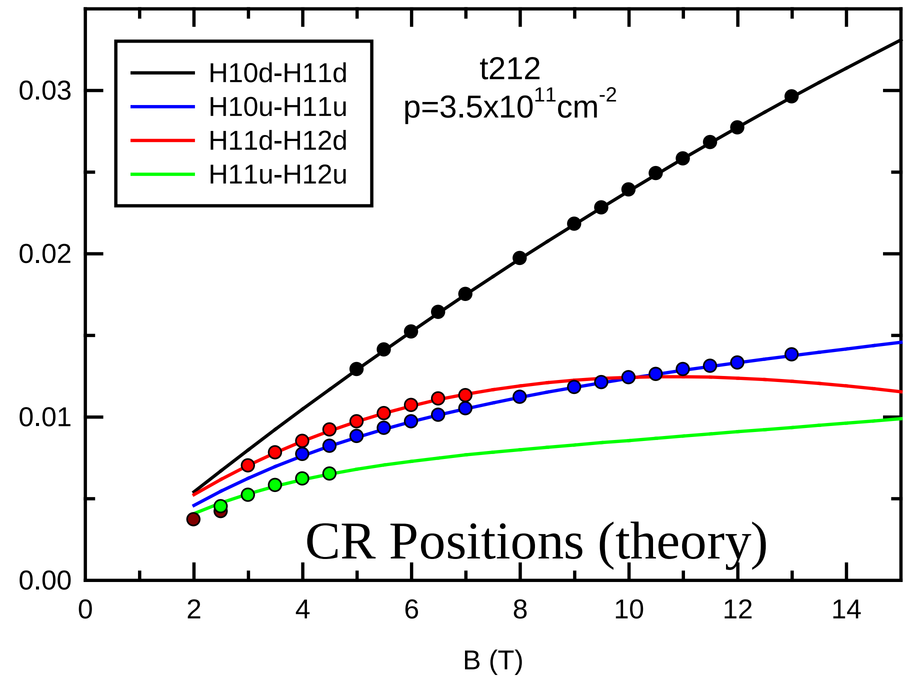

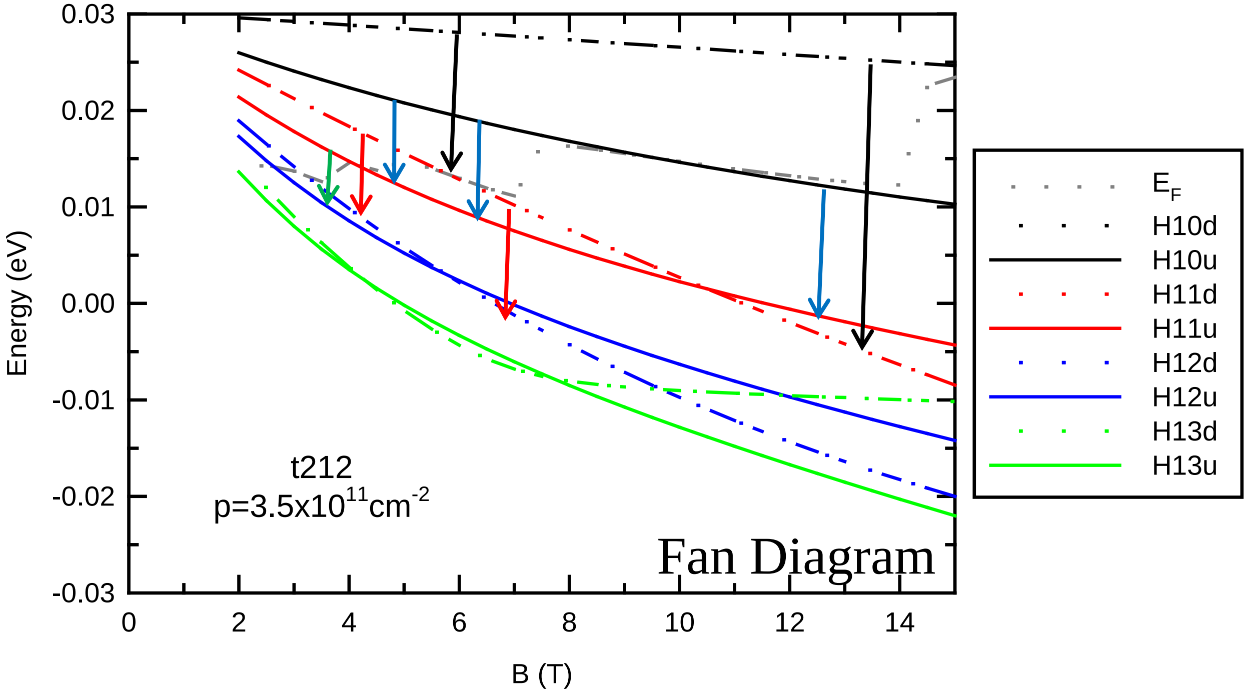

- Good agreement with theory…
- …except for one branch.

Dependence on Hole Density

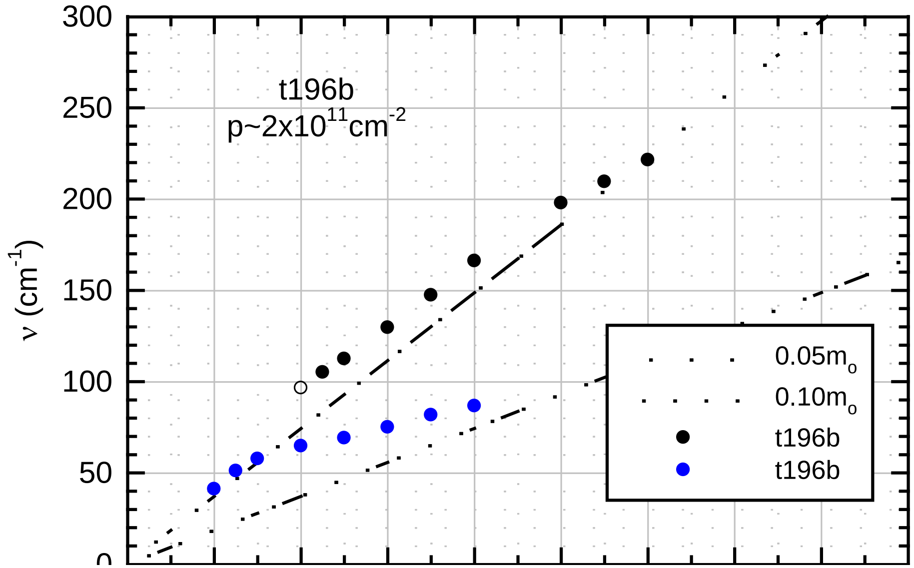

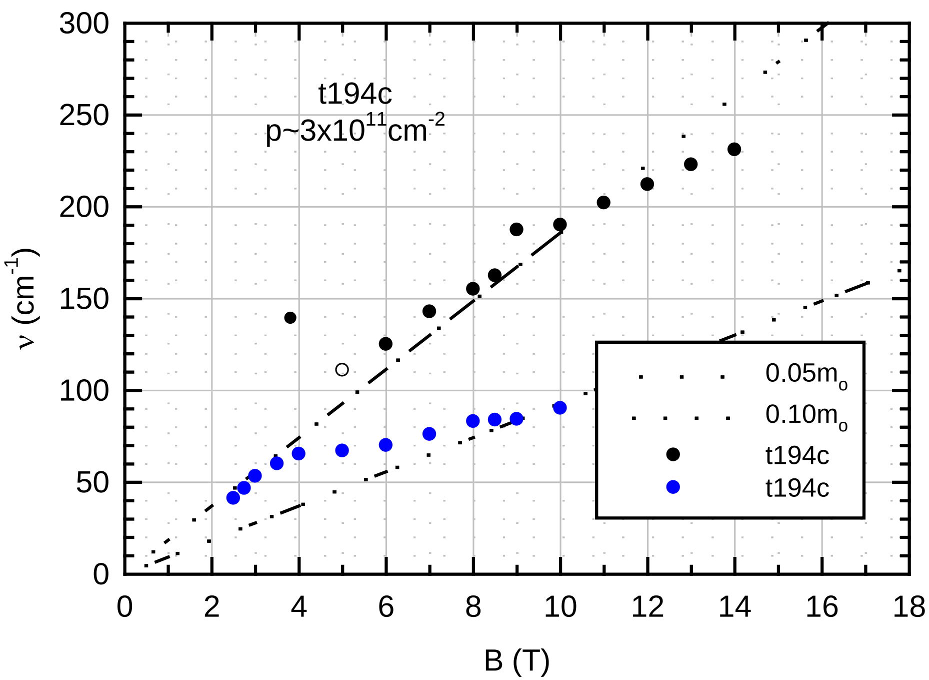

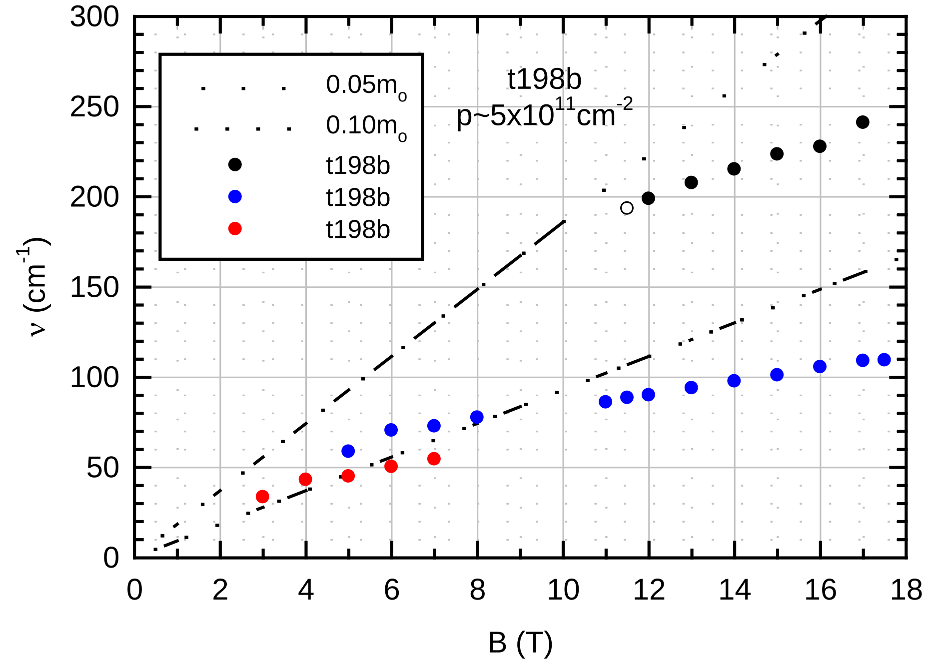

Effective mass increases with increasing hole density.

Summary

Molecular Beam Epitaxy of InSb-based heterostructures

- Mobility partially limited by micro-twins and dislocations
- Defect densities depends on buffer layer composition
- Room temperature mobility as high as 41,000 cm^2/Vs

Electron transport through InSb mesoscopic structures

- Ballistic transport observed at $T{\sim}200K$ in 0.5μm devices
- Quantized conductance observed in point contacts
- Magnetic focusing features observed

2D Hole systems in InSb quantum wells

- Mobility lower than for 2D electron systems
- Cyclotron resonance shows $m^{*} \geq 0.04 m_e$
- Good prototype system for *p*-type III-V quantum wells